

Strategic reconstruction of macrophage-derived extracellular vesicles as a magnetic resonance imaging contrast agent

Sagar Rayamajhi¹, Ramesh Marasini¹, Tuyen Duong Thanh Nguyen¹, Brandon L Plattner³, David Biller², Santosh Aryal^{1*}

¹Department of Chemistry, Nanotechnology Innovation Center of Kansas State (NICKS), Kansas State University, Manhattan, KS 66506, USA

²Department of Clinical Sciences, College of Veterinary Medicine, Kansas State University, Manhattan, KS, 66506, USA

³Department of Diagnostic Medicine and Pathobiology, College of Veterinary Medicine, Kansas State University, Manhattan, KS, 66506, USA

* Corresponding Author

Santosh Aryal, Ph.D.

Department of Chemistry, Kansas State University, Manhattan, KS

Email: saryal@ksu.edu

Phone: 785-532-6326

Fax: 785-532-4953

Supporting Information

Number of pages: 4

Number of figures: 3

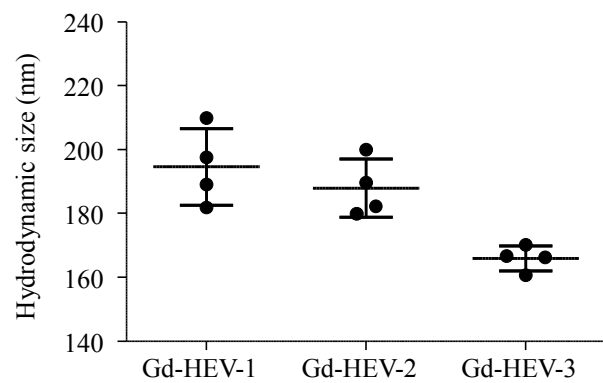


Figure S1: Hydrodynamic size of three different formulations of Gd-HEV with the different molar ratios of constituents. Graph shows hydrodynamic size at four different days for each formulation (days 0, 3, 6, and 10).

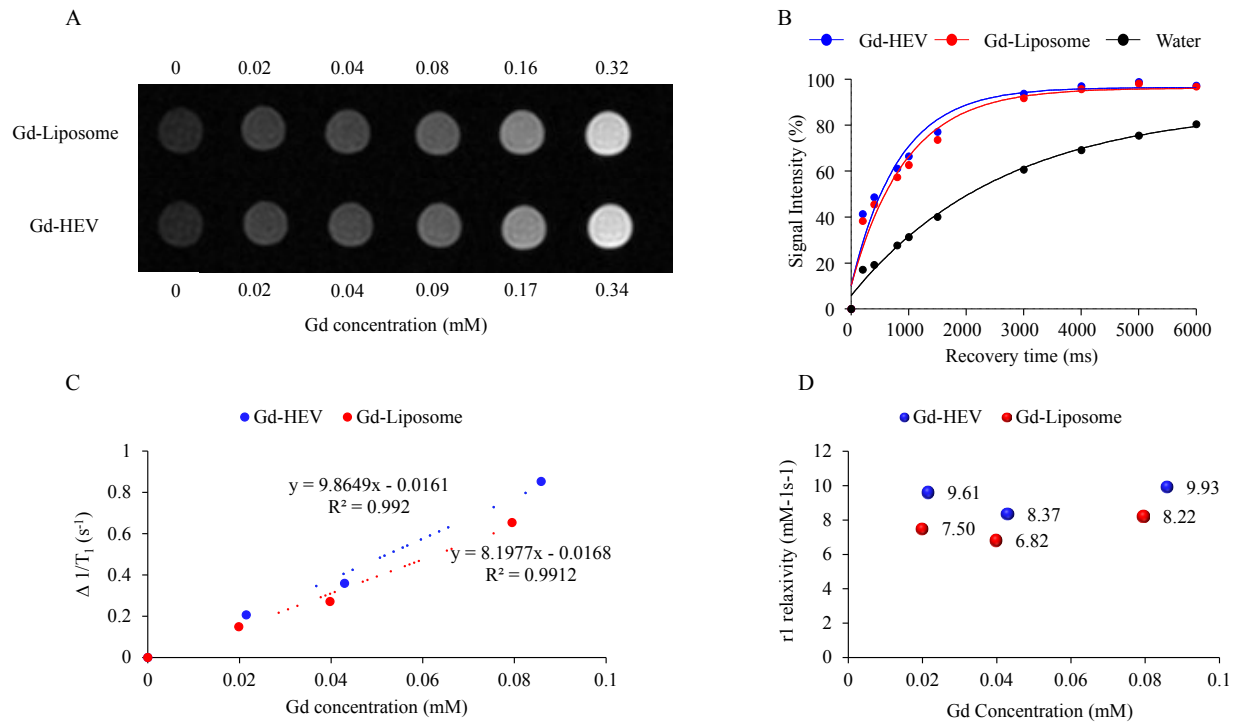


Figure S2: Comparison of magnetic characterization of Gd-HEV and Gd-liposome. (A) T_1 weighted image of Gd-HEV and Gd-Liposome at different Gd concentration showing contrast enhancement in a 3T clinical MRI system (TR=400 ms, TE=10 ms, and slice thickness=2 mm), (B) T_1 recovery curve of Gd-HEV (0.09 mM Gd), Gd-Liposome (0.08 mM Gd), and water in terms of % signal intensity with respect to recovery time (ms) at specific Gd concentration showing different recovery characteristic, (C) Linear fit of inverse of relative change in T_1 recovery time ($(\Delta 1/T_1 (s^{-1}))$) with respect to different Gd concentration (mM) in Gd-HEV and Gd-Liposome (p-value = 0.117 and 0.118, linear regression analysis of slopes and intercept, respectively). Slope of the fitted model gives longitudinal relaxivity (r_1): 9.87 $mM^{-1}s^{-1}$ for Gd-HEV and 8.20 $mM^{-1}s^{-1}$ for Gd-Liposome, (D) r_1 relaxivity of Gd-HEV and Gd-Liposome at different concentration. All data were obtained using a 3T clinical MRI.

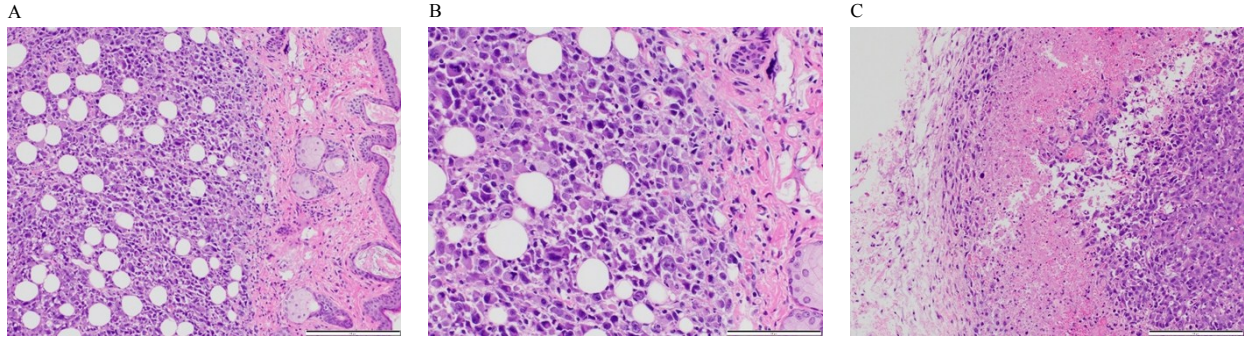


Figure S3: Histologic analysis of tissue sections of the tumor. (A and B) Image showing the dermal anaplastic sarcoma and (C) Image showing the subcutaneous anaplastic tumor along with areas of necrosis and hemorrhage (Scale bar: A-200 μ m, B-100 μ m, C-200 μ m).

Histological features of tumor: Within the dermis and extending through the cutaneous trunci muscle into the subcutaneous adipose tissue is a multilobular and well-demarcated neoplasm composed of neoplastic polygonal to spindle-shaped cells arranged in dense sheets and clusters supported by a fibrovascular stroma. The cells have a moderate amount of eosinophilic cytoplasm, a single large round to oval nucleus with 1-3 prominent magenta or basophilic nucleoli. There is moderate to marked anisocytosis and anisokaryosis; there are increased numbers of mitotic figures (up to 10 figures, some are bizarre) per high powered 40X field of view. Within the dermal nodule, approximately 5% of the mass is necrotic characterized by necrotic karyorrhectic debris. The neoplastic cells extend into the superficial dermal collagen, and also through the underlying skeletal muscle and into the subcutaneous space where they form a distinct nodule. Here, the cell features are similar, though approximately 60% of this nodule is composed of necrotic debris intermixed with degenerate neutrophils and hemorrhage. The nodule is surrounded by loose fibrous connective tissue.